Flux-driven algebraic damping of diocotron modes

Chi Yung Chim and Thomas M. O'Neil

University of California, San Diego, CA 92093, USA

Abstract. Recent experiments with pure electron plasmas in a Malmberg-Penning trap have observed the algebraic damping of $m = 1$ and $m = 2$ diocotron modes. Transport due to small field asymmetries produces a low density halo of electrons moving radially outward from the plasma core, and the mode damping begins when the halo reaches the resonant radius R_m, where there is a matching of $\omega_m = m\omega_E(R_m)$ for the mode frequency ω_m and $\mathbf{E}\times\mathbf{B}$-drift rotation frequency ω_E. The damping rate is proportional to the flux of halo particles through the resonant layer. The damping is related to, but distinct from, spatial Landau damping, in which a linear wave-particle resonance produces exponential damping. This new mechanism of damping is due to transfer of canonical angular momentum from the mode to halo particles, as they are swept around the "cat's eye" orbits of the resonant wave-particle interaction. This paper provides a simple derivation of the time dependence of the mode amplitudes.

Keywords: nonneutral plasma, diocotron mode, Kelvin wave, damping, symmetrization
PACS: 52.27.Jt, 52.35.Kt, 52.35.We, 52.65.Cc

INTRODUCTION

Diocotron modes have long been a topic of study in non-neutral plasmas. They are surface modes on nonneutral plasma columns, and are closely related to Kelvin waves on vorticity patches[1, 2]. Kabantsev *et. al.* recently discovered algebraic damping of the $m = 1$ and $m = 2$ diocotron modes in plasmas where transport drives a low density halo of particles radially outward from the plasma core to the wall[3, 4]. The damping begins when the halo reaches the resonant radius R_m of the modes, where $\omega_m = m\omega_E(R_m)$. Here ω_m is the mode frequency and $\omega_E(r)$ is the $\mathbf{E}\times\mathbf{B}$-drift rotation frequency. The results from the experiments[3] show a linear in time algebraic decrease in mode amplitude

$$D_1(t)/R_w = D_1(0)/R_w - 1.5\Gamma t/N_L, \tag{1}$$
$$D_2(t)/R_p = D_2(0)/R_p - 3.8\Gamma t/N_L, \tag{2}$$

where R_p and R_w are the plasma core and wall radii respectively, D_m is the amplitude of the surface ripple characterizing the m-th mode, N_L is the line density of the core, and the flux Γ is number of particle passing through the resonant layer per unit length and time. This behavior is different from the exponential decrease displayed in spatial Landau damping[1, 5, 6].

This paper provides a simple derivation of the damping rates. As particles are swept across the resonant radius, they gain canonical angular momentum from the mode, and angular momentum balance requires the mode to damp. In our analysis, when particle transport is only due to mobility, we obtain the following solutions for the time dependence of the mode amplitudes

$$D_1(t)/R_w = D_1(0)/R_w - (2/\pi)\frac{\Gamma t/N_L}{1+2n_hR_w^2/(n_0R_p^2)}, \tag{3}$$
$$\frac{2}{3}[\frac{D_2(t)}{R_p}]^{3/2} + 4\frac{n_h}{n_0}[\frac{D_2(t)}{R_p}]^{1/2} = \frac{2}{3}[\frac{D_2(0)}{R_p}]^{3/2} + 4\frac{n_h}{n_0}[\frac{D_2(0)}{R_p}]^{1/2} - \frac{4\sqrt{2}\Gamma t}{\pi N_L}, \tag{4}$$

where n_h and n_0 are the halo and core densities respectively.

DIOCOTRON MODE AND MODE POTENTIAL

A diocotron mode can be thought of as a ripple on the surface of the plasma core. Here we assume a plasma core with uniform density $n_0 \sim 10^7$ cm^{-3} and a radius $R_p \simeq 1.3$ cm. Such a core has a line density $N_L = \pi n_0 R_p^2$. Each electron

carries a charge $e = -|e|$. The surface radius of the core varies as

$$r(\theta,t) = R_p + D_m \cos(m\theta - \omega_m t - \alpha_m), \tag{5}$$

where D_m is the amplitude of the ripple of mode number m, α_m is the initial phase angle of the mode, and ω_m is the mode frequency. We consider the limit where D_m is small, and describe such a displacement by a delta-function type variation of the core density at the surface:

$$n(r,\theta,t) = n_0\Theta(R_p - r) + n_0 D_m \delta(r - R_p)\cos(m\theta - \omega_m t - \alpha_m). \tag{6}$$

This density distribution sets up an electric potential ϕ that follows from Poisson's equation $\nabla^2\phi = -4\pi ne$ and the boundary condition $\phi = 0$ at the wall radius $R_w \simeq 3.5$ cm. The unperturbed potential is

$$\phi_0(r) = \begin{cases} N_L e \ln(R_w^2/r^2) & (r > R_p) \\ N_L e[\ln(R_w^2/R_p^2) + 1 - r^2/R_p^2] & (r < R_p) \end{cases}, \tag{7}$$

and the mode potential due to the surface displacement is[7]

$$\phi_m(r) = \begin{cases} -\dfrac{2N_L e}{m}\left(\dfrac{D_m}{R_p}\right)\left(\dfrac{rR_p}{R_w^2}\right)^m\left[1 - \left(\dfrac{R_w}{r}\right)^{2m}\right] & (r > R_p) \\ -\dfrac{2N_L e}{m}\left(\dfrac{D_m}{R_p}\right)\left(\dfrac{rR_p}{R_w^2}\right)^m\left[1 - \left(\dfrac{R_w}{R_p}\right)^{2m}\right] & (r < R_p) \end{cases}. \tag{8}$$

The total potential is $\phi(r,\theta,t) = \phi_0(r) + \phi_m(r)\cos(m\theta - \omega_m t - \alpha_m)$.

For a "top hat" radial density profile, the diocotron mode frequency is given by the expression[7]

$$\omega_m = \omega_E(R_p)\left[(m-1) + \frac{R_p^{2m}}{R_w^{2m}}\right], \tag{9}$$

where $\omega_E(r)$ is the $\mathbf{E}\times\mathbf{B}$-drift rotation frequency due to the unperturbed core. Note that $\omega_E(R_p) = -2\pi n_0 ec/B \simeq 7.5\times10^4$ s^{-1} for $B = 12$ kG, and $\omega_E(r) = \omega_E(R_p)\cdot(R_p^2/r^2)$ for $r > R_p$, i.e. outside the core. For the $m = 1$ mode, $\omega_1 = \omega_E(R_p)(R_p/R_w)^2 = \omega_E(R_w)$. For the $m = 2$ mode, we take the limit $R_p/R_w \to 0$, and thus $\omega_2 = \omega_E(R_p)$. Thus, from the expression $\omega_m = m\omega_E(R_m)$, the resonant radii for the $m = 1$ and $m = 2$ modes are given by

$$R_1 = R_w, \tag{10}$$

$$R_2 = \sqrt{2}R_p. \tag{11}$$

PARTICLE MOTION

In the regime where diocotron modes are studied, inertial effects of electrons are neglected, and they are described by the motion of their guiding centers under $\mathbf{E}\times\mathbf{B}$ drifts[7]. The equations of motion of a guiding center, in the polar coordinates (r,θ), is

$$\frac{dr}{dt} = -\frac{c}{rB}\frac{\partial\phi}{\partial\theta}, \tag{12}$$

$$\frac{d\theta}{dt} = \frac{c}{rB}\frac{\partial\phi}{\partial r}, \tag{13}$$

where $\phi(r,\theta)$ is the electric potential at the point (r,θ), and B is the magnetic field strength. The z-axis is taken to be the direction that the magnetic field points in.

By defining $P_\theta = eBr^2/(2c)$, and $H = e\phi$, eqns. (12) and (13) are rewritten as

$$\frac{dP_\theta}{dt} = -\frac{\partial H}{\partial\theta}, \tag{14}$$

$$\frac{d\theta}{dt} = \frac{\partial H}{\partial P_\theta}. \tag{15}$$

In this formulation, H is a Hamiltonian and (θ, P_θ) is a canonically conjugate pair.

In the laboratory frame, the Hamiltonian is given by the expression

$$H(\theta, P_\theta) = e\phi_0(r(P_\theta)) + e\phi_m[r(P_\theta)), t]\cos(m\theta - \omega_m t - \alpha_m). \tag{16}$$

There are two time dependences in this Hamiltonian. There is the rapid time dependence associated with the propagation of the wave, that is, the term $\omega_m t$ in the argument of the cosine, and there is the slow time dependence in $\omega[r(P_\theta), t]$ associated with the slow damping of the wave. We remove the rapid time dependence by making a canonical transformation to the wave-rotating frame with the generating function $F(\theta, \bar{P}_\theta, t) = \bar{P}_\theta(m\theta - \omega_m t - \alpha_m)$[8]. From the generating function, we obtain the transformation

$$\bar{\theta} = \theta - \frac{1}{m}(\omega_m t + \alpha_m), \bar{P}_\theta = P_\theta, \tag{17}$$

where the new Hamiltonian is given by

$$\bar{H} = H + \frac{\partial F}{\partial t} = H - \frac{\omega_m}{m}P_\theta = e\phi_0[r(P_\theta)] + e\phi_m[r(P_\theta), t]\cos\bar{\theta}. \tag{18}$$

We assume that the remaining time dependence in $\phi_m[r(P_\theta), t]$ is sufficiently slow that it can neglected on the orbit time scale. A particle then stays on a contour of constant $\bar{H}$ in the mode-rotating frame.

We are interested in the dynamics near the resonance radius R_m, where $\omega_m = m\omega_E(R_m) = m(c/R_m B)(\partial\phi_0/\partial r)_{R_m}$. We expand $\bar{H}$ to the lowest order of $P_\theta - P_m$, where $P_m = eBR_m^2/(2c)$ is the canonical angular momentum at resonant radius R_m, and omit constant terms as they do not affect the dynamics.

For the $m = 1$ mode, $P_1 = P_w \equiv eBR_w^2/(2c)$. In the mode-rotating frame, the Taylor-expanded Hamiltonian with the mode is

$$\bar{H}(\bar{\theta}, P_\theta) = \frac{N_L e^2}{2}[(\frac{P_\theta - P_w}{P_w})^2 - 4\frac{D_1}{R_w}(\frac{P_\theta - P_w}{P_w})\cos\bar{\theta}]. \tag{19}$$

For the $m = 2$ mode, the mode-rotating Hamiltonian is expanded as

$$\bar{H}(\bar{\theta}, P_\theta) = \frac{N_L e^2}{2}[(\frac{P_\theta - P_2}{P_2})^2 + \frac{D_2}{R_p}\cos 2\bar{\theta}]. \tag{20}$$

For each mode, the constant Hamiltonian contours form a cat's-eye at the resonant radius. The cat's-eye is a separatrix between the closed contours inside and open contours outside. The separatrix can be split into two parts. The radially outer part with larger values of P_θ is defined by $P_\theta = P_{m+}(\bar{\theta})$, as one sweeps through the angle $\bar{\theta}$, and the inner part is defined by $P_\theta = P_{m-}(\bar{\theta})$.

For the $m = 1$ mode, the separatrix is the contour of $\bar{H} = 0$. By solving eqn. (19) at $\bar{H} = 0$, the outer part is

$$P_{1+}(\bar{\theta}) = P_w, \tag{21}$$

which is at the wall, and the inner part is

$$P_{1-}(\bar{\theta}) = P_w(1 + 4\frac{D_1}{R_w}\cos\bar{\theta}) \tag{22}$$

for $\pi/2 < \bar{\theta} < 3\pi/2$. In Fig. (1) we display the separatrix for $m = 1$ with a thick line, and other contours with dashed lines. The cat's-eye shape of the separatrix is distorted and asymmetric in P_θ, since the resonant radius is at the wall, where the potential goes to zero.

For the $m = 2$ mode, the separatrix is the contour $\bar{H} = N_L e^2(D_2/R_p)/2$. By solving that using eqn.(20), the separatrix corresponds to

$$P_{2\pm}(\bar{\theta}) = P_2(1 \pm \sqrt{2\frac{D_2}{R_p}|\sin\bar{\theta}|}). \tag{23}$$

In Fig. (2) we display the separatrix for $m = 2$ with a thick line, and other contours with dashed lines. The separatrix takes the shape of a symmetric cat's-eye.

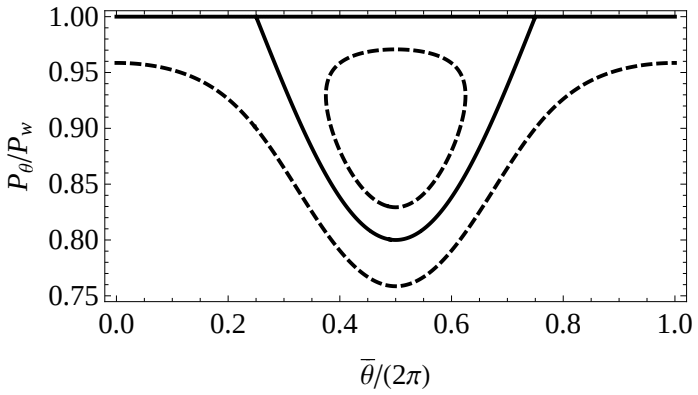

FIGURE 1. Contours of the $m = 1$ mode potential. The separatrix is in solid line and other contours are in dashed lines.

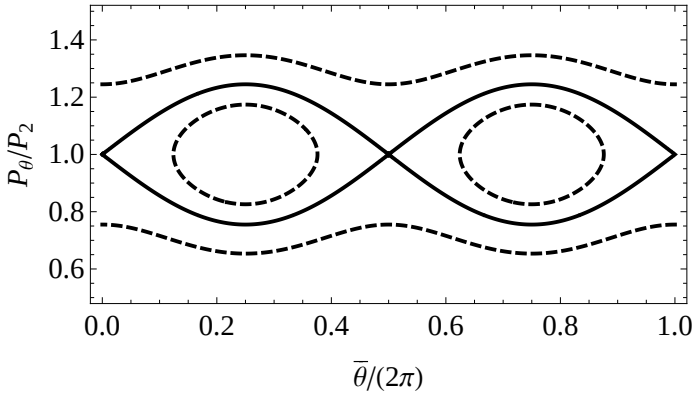

FIGURE 2. Contours of the $m = 2$ mode potential. The separatrix is in solid line and other contours are in dashed lines.

MODE DAMPING

The electron plasma core is confined in a Malmberg-Penning trap and rotates with the $\mathbf{E}\times\mathbf{B}$-drift frequency. When field asymmetries are introduced, a dilute flux of halo of density $n_h \sim 10^{-2} n_0$ eminates from the core and propagates towards the wall with a radial flow velocity $v_r \sim 10^{-2}$ cm s^{-1}[3, 4]. We assume the particle transport is due to mobility flow, and neglect diffusion. The flux Γ, which is the number of particles flowing across a radius per unit time, is given by

$$\Gamma = 2\pi n_h r v_r. \tag{24}$$

Experimentally, Γ/N_L is typically 10^{-3} s^{-1}. By adjusting the field asymmetry, v_r and thus Γ vary. For such a radial flow velocity, there is an associated flow velocity $\dot{P}_\theta|_T = eBrv_r/c$ in P_θ-direction.

We assume that during the movement of a particle, D_1 and D_2 are essentially fixed. As a particle reaches the the separatrix at angle $\bar{\theta}$, it is swept around the cat's eye by the field potential and makes a step $\Delta P_\theta(\bar{\theta})$. For the $m = 1$ mode, the step size is simply the difference between the inner curve of the separatrix and the wall, and that gives

$$\Delta P_\theta(\theta) = \begin{cases} -4P_w(D_1/R_w)\cos\bar{\theta} & (\pi/2 < \bar{\theta} < 3\pi/2) \\ 0 & (\text{otherwise}) \end{cases}. \tag{25}$$

For the $m = 2$ mode, we notice that the separatrix is symmetric about $P_\theta = P_2$. We assume a low mode amplitude such that the separatrix width is small. Then around the separatrix $\dot{P}_\theta|_T$ can be taken as a constant, and the particle spends the same amount of time on both sides of the separatrix as it is swept around. As a result, the particle enters and leaves the separatrix at the same angle $\bar{\theta}$. Therefore, the step size is the difference between $P_{2+}(\bar{\theta})$ and $P_{2-}(\bar{\theta})$,

which is

$$\Delta P_\theta(\theta) = 2P_r\sqrt{2D_2/R_p}|\sin\bar{\theta}|. \tag{26}$$

As a particle is swept around the separatrix, it makes a radial step $\Delta r = c\Delta P_\theta/(eBr)$. For $m = 1$ mode the step size is of the order $D_1 \sim 0.3$ cm, and for $m = 2$ the step size is of the order $R_2\sqrt{D_2/R_p} \sim 2\text{ cm}\sqrt{0.04} = 0.4$ cm. The timescale of the particle being swept around is $1/\omega_E(R_m) \sim 10^{-4}$ s, and the radial velocity of the mobility flow is $v_r \sim 0.01$ cm s^{-1} as the particle is pushed towards the wall by mobility. In this timescale, the gain in radial position due to mobility is $\delta r \sim v_r/\omega_E(R_m)$, which is of the scale 10^{-6} cm, which is much smaller than the radial step $\Delta r \sim 0.1$ cm. The gain in angular momentum, therefore, is primarily due to the diocotron mode through the mode potential.

As particles make the radial steps Δr across the separatrix, the mode loses angular momentum to the particles as angular momentum is conserved. The mode angular momentum per unit length is $P_{\text{mode}} = N_L eBD_m^2/(2c)$ for the mode number m[1]. As angular momentum is lost in the mode to the particles, the mode amplitude D_m decreases slowly in time, i.e. the mode damps. Note that the analysis of damping in this paper excludes the effects of interaction between halo particles, mode harmonics or frequency shifts. Studies of those effects, and damping in relation to the detailed density distribution of the halo are in progress.

The rate that particles are brought to the separatrix is the flux Γ. By taking average of ΔP_θ over all the incident angles on the separatrix, the rate of angular momentum transfer to the particles taking the step ΔP_θ is $\Gamma\int_0^{2\pi} d\bar{\theta}\Delta P_\theta/(2\pi)$. Balancing with the mode angular momentum, the rate equation of the mode amplitude is

$$\frac{d}{dt}N_L\frac{eB}{2c}D_m^2 + \Gamma\int_0^{2\pi}\frac{d\bar{\theta}}{2\pi}\Delta P_\theta = 0. \tag{27}$$

The rate equations above assume a stationary mode potential when the angular momentum gain of the particles is calculated. However, the flux of particle entering the separatrix decreases as mode damps and the separatrix shrinks in size. An ad-hoc method to take the flux decrease into account is to calculate the the effective flux by the flow velocity $\dot{P}_\theta|_T$ of a particle relative to the shrinking velocity $\dot{P}_{m-}$ of the separatrix. The effective flux per unit angle is given by

$$\Gamma_{\text{eff}}(\bar{\theta}) = \frac{\Gamma}{2\pi}\left(\frac{\dot{P}_\theta|_T - \dot{P}_{m-}}{\dot{P}_\theta|_T}\right), \tag{28}$$

and the corrected rate equation of the mode amplitude is

$$\frac{d}{dt}N_L\frac{eB}{2c}D_m^2 + \int_0^{2\pi} d\bar{\theta}\Gamma_{\text{eff}}(\bar{\theta})\Delta P_\theta = 0. \tag{29}$$

For $m = 1$ mode, the inner part of the separatrix increases its angular momentum at a rate

$$\dot{P}_{1-} = 4P_w\frac{\dot{D}_1}{R_w}\cos\bar{\theta} \tag{30}$$

for the angle range $\pi/2 < \bar{\theta} < 3\pi/2$. The resulting damping equation from eqns. (28) to (30) is

$$\frac{\dot{D}_1}{R_w} = -\frac{2}{\pi}\frac{\Gamma}{N_L}\left(1 + 2\frac{n_h}{n_0}\frac{R_w^2}{R_p^2}\right)^{-1}. \tag{31}$$

A trivial integration of eqn. (31) shows that the mode amplitude decreases linearly with time, i.e.

$$D_1(t) = D_1(0) - R_w\cdot\frac{2}{\pi}\frac{\Gamma t/N_L}{1 + 2(n_h R_w^2)/(n_0 R_p^2)}. \tag{32}$$

We plot in Fig. (3) the amplitude profile of the $m = 1$ mode as time progresses. We set $n_h/n_0 = 10^{-2}$, and $\Gamma/N_L = 2\times 10^{-3}$ s^{-1}. The curve from the theoretical derivation is in a solid line, and the linear curve from experimentally observed damping rate is in a dashed line. The figure shows that the simple theory agrees with the experiment qualitatively. The theory however shows a slower damping, and the reason is yet to be discovered.

For $m = 2$ mode, the inner part of the separatrix increases its angular momentum at a rate

$$\dot{P}_{2-} = -P_r\frac{\dot{D}_2}{\sqrt{2D_2R_p}}|\sin\bar{\theta}|. \tag{33}$$

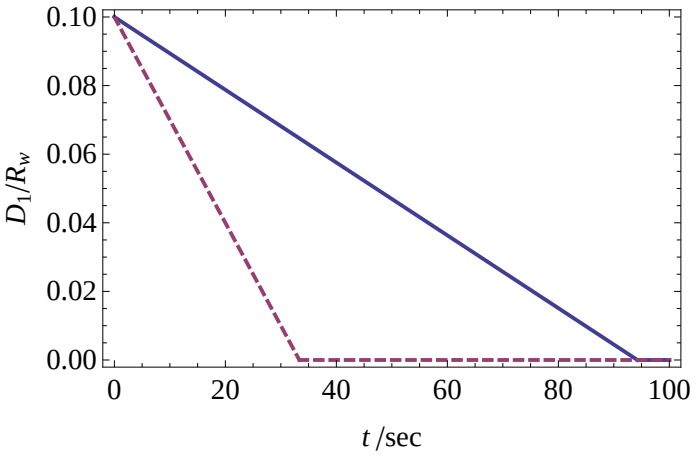

FIGURE 3. Damping curve of the $m = 1$ mode amplitude D_1/R_w. The theoretical result is in a solid line, and the dashed line is the curve using the rate from experimental observation.

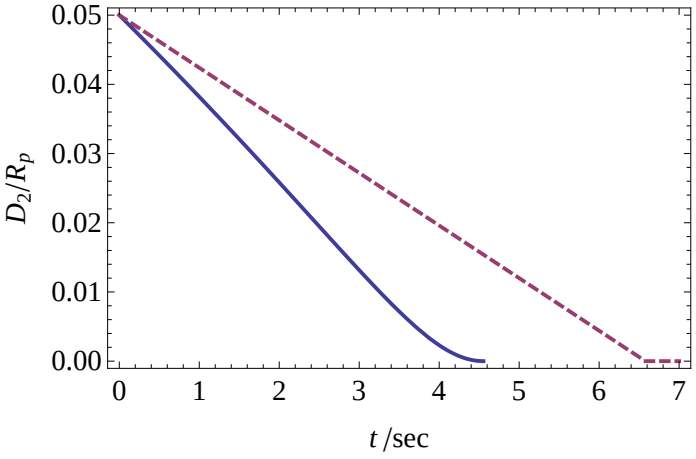

FIGURE 4. Damping curve of the $m = 2$ mode amplitude D_2/R_p. The theoretical result is in a solid line, and the dashed line is the curve using the rate from experimental observation.

The resulting damping equation from eqns. (28), (29) and (33) is

$$\frac{\dot{D}_2}{R_p}\left(\frac{D_2}{R_p}+2\frac{n_h}{n_0}\right) = -\frac{4\sqrt{2}}{\pi}\frac{\Gamma}{N_L}\left(\frac{D_2}{R_p}\right)^{1/2}. \tag{34}$$

If the mode amplitude is large, i.e. $D_2(t)/R_p \gg n_h/n_0$, the mode damping occurs at an increasing rate as the amplitude drops, since $\dot{D}_2/R_p \simeq -(4\sqrt{2}/\pi)(\Gamma/N_L)(D_2/R_p)^{-1/2}$. However, when the mode amplitude is small, i.e. $D_2(t)/R_p \ll n_h/n_0$, the damping rate slows down and approaches zero at zero amplitude, i.e. the damping curve becomes flat, since then $\dot{D}_2/R_p \simeq -(2\sqrt{2}/\pi)(\Gamma/N_L)(D_2/R_p)^{1/2}/(n_h/n_0)$. The implicit solution from integration of eqn. (34) is

$$\frac{2}{3}\left[\frac{D_2(t)}{R_p}\right]^{3/2}+4\frac{n_h}{n_0}\left[\frac{D_2(t)}{R_p}\right]^{1/2} = \frac{2}{3}\left[\frac{D_2(0)}{R_p}\right]^{3/2}+4\frac{n_h}{n_0}\left[\frac{D_2(0)}{R_p}\right]^{1/2}-\frac{4\sqrt{2}\Gamma t}{\pi N_L}. \tag{35}$$

We plot in Fig. (4) the time dependence of the $m = 2$ mode amplitude. We set the same values of n_h/n_0 and Γ/N_L as in Fig. (3). The curve from the theoretical derivation is in a solid line, and the linear curve from experimentally observed damping rate is in a dashed line. The figure shows that the simple theory agrees with the experiment qualitatively, and the damping times are of the same order of magnitude. As the initial amplitude $D_2/R_p = 5\times 10^{-2}$

is of the same order of magnitude as the density ratio $n_h/n_0 = 10^{-2}$, the damping, in theory, does not speed up as the amplitude decreases, and during most of the damping time, shows a damping behavior similar to the linear time-dependence in the experimental observation. Then at the end of the damping, the amplitude is so small that the damping rate approaches zero and the curve becomes flat.

In short, we derive the damping curve of the $m = 1$ and $m = 2$ modes with conservation of canonical angular momentum. When particles from the mobility flux are swept across the separatrix, they gain angular momentum from the mode and make radial steps across separatrix. The mode damps as a result. The damping curves are similar to experimental observations qualitatively, and the damping times from theory and from experiment are of the same scale.

ACKNOWLEDGMENTS

This work was supported by NSF/DOE Partnership grants PHY-1414570 and DE-SC0002451.

REFERENCES

1. D. Schecter, D. Dubin, A. Cass, C. Driscoll, I. Lansky, and T. O'Neil, *Phys. Fluids* **12**, 2397–2412 (2000).
2. N. Balmforth, S. G. Llewellyn Smith, and W. Young, *J. Fluid Mech.* **426**, 95–133 (2001).
3. A. A. Kabantsev, C. Y. Chim, T. M. O'Neil, and C. F. Driscoll, *Phys. Rev. Lett.* **112**, 115003 (2014).
4. A. A. Kabantsev, T. M. O'Neil, and C. F. Driscoll, "Algebraic damping of diocotron waves by a flux of particles through the wave resonant layer," in *NON-NEUTRAL PLASMA PHYSICS VIII: 10th International Workshop on Non-Neutral Plasmas*, AIP Publishing, 2013, vol. 1521, pp. 35–42.
5. J. Danielson, F. Anderegg, and C. Driscoll, *Phys. Rev. Lett.* **92**, 245003 (2004).
6. F. F. Chen, *Introduction to Plasma Physics and Controlled Fusion*, Plenum Press, New York, 1984, vol. 1, pp. 240–261, 2nd edn.
7. R. C. Davidson, *Physics of Nonneutral Plasmas*, Imperial College Press, London, 2001, pp. 289–343.
8. H. Goldstein, C. Poole, and J. Safko, *Classical Mechanics*, Addison Wesley, San Francisco, 2002, pp. 368–375, 3rd edn.